Use of a Cryptic Splice Site for the Expression of Huntingtin Interacting Protein 1 in Select Normal and Neoplastic Tissues

Chiron W. Graves, Steven T. Philips, Sarah V. Bradley, Katherine I. Oravecz-Wilson, Lina Li, Alice Gauvin, and Theodora S. Ross

Department of Internal Medicine, University of Michigan Medical School, Ann Arbor, Michigan

Abstract

Huntingtin interacting protein 1 (HIP1) is a 116-kDa endocytic protein, which is necessary for the maintenance of several tissues *in vivo* as its deficiency leads to degenerative adult phenotypes. HIP1 deficiency also inhibits prostate tumor progression in mice. To better understand how deficiency of HIP1 leads to such phenotypes, we analyzed tumorigenic potential in mice homozygous for a *Hip1* mutant allele, designated *Hip1*$^{\Delta 3\text{-}5}$, which is predicted to result in a frame-shifted, nonsense mutation in the NH_2 terminus of HIP1. In contrast to our previous studies using the *Hip1* null allele, an inhibition of tumorigenesis was not observed as a result of the homozygosity of the nonsense Δ3-5 allele. To further examine the contrasting results from the prior *Hip1* mutant mice, we cultured tumor cells from homozygous Δ3-5 allele–bearing mice and discovered the presence of a 110-kDa form of HIP1 in tumor cells. Upon sequencing of *Hip1* DNA and message from these tumors, we determined that this 110-kDa form of HIP1 is the product of splicing of a cryptic U12-type AT-AC intron. This event results in the insertion of an AG dinucleotide between exons 2 and 6 and restoration of the reading frame. Remarkably, this mutant protein retains its capacity to bind lipids, clathrin, AP2, and epidermal growth factor receptor providing a possible explanation for why tumorigenesis was not altered after this knockout mutation. Our data show how knowledge of the transcript that is produced by a knockout allele can lead to discovery of novel types of molecular compensation at the level of splicing. [Cancer Res 2008;68(4):1064–73]

Introduction

Huntingtin interacting protein 1 (HIP1) was first identified by its ability to interact with huntingtin, the protein encoded by the gene that is mutated in Huntington's disease (1, 2). HIP1 and its only known mammalian relative, HIP1-related (HIP1r), were subsequently shown to specifically interact with clathrin, AP2 (3–10), and epidermal growth factor receptor (EGFR; ref. 11). Thus, the HIP1 family is widely thought to be involved in the regulation of growth factor receptor endocytosis and signaling. Additionally, HIP1 and HIP1r contain AP180 N-terminal homology (ANTH) inositol lipid-binding domains, which are specific to endocytic proteins (12, 13). Finally, deficiency of HIP1 leads to spinal defects, testicular degeneration, cataracts, adult weight loss, and early death (14–16). These *in vivo* phenotypes indicate that HIP1 is necessary for fundamental cellular and organismal homeostasis. Despite their clear necessity in the maintenance of adult cells and tissues, the precise cellular and biochemical function(s) of this protein family are yet to be determined. In fact, several attempts at understanding the effects of HIP1/HIP1r deficiency on receptor endocytosis either in cultured cells or *in vivo* have not been successful (14, 16, 17).

In addition to its function in normal tissue maintenance, HIP1 has been widely implicated in tumorigenesis. HIP1 was discovered to be an amino terminal partner of platelet-derived growth factor β receptor (PDGFβR) in the leukemogenic fusion resulting from a *t*(5;7) chromosomal translocation (18). HIP1 protein has also been found to be up-regulated in multiple human tumor types, including prostate, colon (19), breast (20), brain (11), and lymphoid (21) cancers. Additionally, HIP1 overexpression is prognostic in prostate cancer (19). Furthermore, heterologous human HIP1 overexpression can transform mouse fibroblasts (20), an effect that we propose to be due to altered growth factor receptor endocytosis and subsequent signal transduction cascades.

To examine the role of HIP1 in prostate cancer, we have previously used mutant mice that are deficient in HIP1 due to a spontaneous targeting event (*Hip1*^{null}). When these HIP1-deficient mice were crossed with the transgenic adenocarcinoma of mouse prostate (TRAMP) mice (22), the HIP1-deficient progeny mice contained fewer and less aggressive prostate tumors than their littermate TRAMP control mice (23). We have expanded these studies by using a different tumor model system (MMTV-MYC model of breast cancer) and a third generation *Hip1* knockout mouse allele (*Hip1*$^{\Delta 3\text{-}5}$) that does not provide the confounding issues associated with the above-described spontaneous null allele (16), such as possible altered expression of *HIP1*-neighboring genes caused by the neomycin cassette. In the present study, we report the surprising result that *Hip1*$^{\Delta 3\text{-}5/\Delta 3\text{-}5}$ is equally, if not more, prone to the development of prostate and breast tumors than *Hip1* wild-type mice. Furthermore, we found that the tumor cells from the *Hip1*$^{\Delta 3\text{-}5/\Delta 3\text{-}5}$ genetic background express a truncated form of the Hip1 protein that is the result of a novel cryptic splicing event. These results have important implications not only for the role of HIP1 and its interacting proteins in normal and neoplastic cell biology but also for the development and analysis of mouse model systems with specific targeting events. Our data emphasize the value of how sequencing the transcript that is actually produced by an engineered knockout allele can reveal novel types of molecular compensation at the level of splicing.

Materials and Methods

Mice. Mx1-Cre [B6.Cg-Tg(Mx1-Cre)1Cgn/J, The Jackson Laboratory], *Hip1*^{null}, *Hip1*^{loxp}, *Hip1*$^{\Delta 3\text{-}5}$ (16), TRAMP (C57BL/6, The Jackson Laboratory;

Note: Supplementary data for this article are available at Cancer Research Online (http://cancerres.aacrjournals.org/).

C.W. Graves and S.T. Philips contributed equally to this work.

Requests for reprints: Theodora S. Ross, University of Michigan 6322 CCGC, 1500 East Medical Center Drive, Ann Arbor, MI 48109-0942. Phone: 734-615-5509; Fax: 734-647-9271; E-mail: tsross@umich.edu.

doi:10.1158/0008-5472.CAN-07-5892

ref. 22) and MMTV-myc (MammJ/FVB, gift from Lewis Chodosh; ref. 24) allele-containing mice were maintained and bred under specific pathogen-free conditions as per University Committee on Use and Care of Animals guidelines at University of Michigan. The TRAMP and MMTV-myc allele-containing mice were maintained on pure genetic backgrounds. Because the other alleles were maintained on a mixed C57BL/6;129svj background, all experiments were performed using the appropriate littermate controls.

Tumor analysis in MMTV-myc mice. MMTV-myc transgenic mice were mated onto *Hip1*$^{null/null}$ and *Hip1*$^{\Delta 3\text{-}5/\Delta 3\text{-}5}$ backgrounds and were palpated for breast tumors weekly. Tumor size was measured with calipers. The mice were sacrificed at 1 year of age or if a tumor impeded movement or ulcerated.

Tumor cell culture. Fresh tumor samples from MMTV-myc and TRAMP mice were cut into 1-mm sections, added to DMEM containing 2.2 mg/mL collagenase (Sigma), and incubated for 1 h at 37°C with agitation every 10 min. The digested samples were filtered through a 100-μm nylon cell strainer (Falcon) then centrifuged at 1,000 rpm for 10 min. The supernatant was removed, and the remaining cells were suspended in DMEM/10% fetal bovine serum and plated onto 10-mm dishes. Cells were passaged every 3 days into fresh media.

Genomic DNA sequencing. High-fidelity PCR amplification of the 3-kb genomic region between exons 2 and 6 of *Hip1* from a MMTV-myc; *Hip1*$^{\Delta 3\text{-}5/\Delta 3\text{-}5}$ tumor was performed. The resulting products were cloned, and single-run complete sequencing was performed on two independent clones.

Sequence analysis. The alignment of sequences from wild-type *Hip1* cDNA or MMTV-myc;*Hip1*$^{\Delta 3\text{-}5/\Delta 3\text{-}5}$ tumor genomic DNA was analyzed using a combination of Sequencer version 4.5 (GeneCodes) and National Center for Biotechnology Information BLAST program.

Reverse transcriptase–PCR. Reverse transcription–PCR (RT-PCR) was performed on total RNA using the SuperScript One-Step RT-PCR system (Invitrogen) and primers specific to *Hip1* exon 1 (5′-ATGAAGCAGGTATC-CAACCCGCTGCCC-3′, forward primer) and the exon 14/15 junction (5′-ATTAGCCTGGGCCTTTCTTTCTATCTC-3′, reverse primer) of murine *Hip1* cDNA. Resulting products were separated on 0.8% agarose gels. Products were extracted from the gel and amplified by nested PCR using primers specific to the exon 1/2 junction (5′-TTCGAGCGGACTCAGACGGT-CAGCGTC-3′, forward primer) and the exon 13/14 junction (5′-ATGGCCC-GCTGGCTCTCAATCTTCATG-3′, reverse primer) of murine *Hip1* cDNA. Products were again run on 0.8% agarose gels, extracted, and directly sequenced using the PCR primers that were used for the amplification. PCR products that did not yield readable sequence were cloned using the TOPO TA Cloning Kit for Sequencing (Invitrogen). Multiple clones were selected, and plasmid DNA was isolated and sequenced.

Polyinosinic-polycytidylic treatment of Mx1-Cre mice. Mice were injected i.p. with 250 μg per mouse of polyinosinic-polycytidylic acid (pIpC; Sigma) every other day for 7 or 14 days as previously described (25, 26).

Bone marrow culture. Mouse bone marrow cell monocytic culture was carried out as previously described (14), except that RPMI 1640 and M-CSF (1 ng/mL, Sigma) was used and femur bone marrow was plated onto 100-mm dishes. One week later, cells were directly lysed in the dishes and collected for protein analysis.

Generation of HIP1 expression constructs. Generation of the pcDNA3/FL HIP1 expression construct was reported previously (19). PCR mutagenesis using pcDNA3/FLHIP1 as a template was used to generate the insert for the pcDNA3/hHIP1Δ3-5/insAG expression construct. Two initial PCR products were generated using two separate pairs of primers. The first primer pair consisted of a forward primer specific to exon 1 (5′-AGGGAGACCCAAGCTTGGTA-3′including a *Kpn*I restriction site) and an engineered reverse primer (5′-GGGATTCTTTCTGGCGTGTTTTTCCTT-3′) consisting of sequence from exon 2, an AG dinucleotide, and sequence from the 5′ portion of exon 6. The second primer pair consisted of an engineered forward primer (5′-AACACGCCAGAAAGAATCCCAGGTTCC-3′) consisting of sequence from the 3′ portion of exon 2, an AG dinucleotide, and sequence from exon 6 and a reverse primer specific to exon 14 (5′-TTCTATCTCAGACAGGCTCC-3′; just 3′ of the *Eco*RI restriction site at position 1,290 of the coding sequence). The resulting PCR products were used as templates in a second PCR reaction to generate the hHIP1Δ3-5/insAG insert. The hHIP1Δ3-5/insAG insert was cloned into pcDNA3/FL HIP1 using the *Kpn*I and *Eco*RI restriction sites.

Generation and purification of glutathione *S*-transferase fusion proteins. The 5′ portions of pcDNA3/FLHIP1 and pcDNA3/hHIP1Δ3-5/insAG were cloned into pGEX4T.1 to generate glutathione *S*-transferase (GST)-HIP1wt (amino acids 1–430) and GST-HIP1Δ3-5 (amino acids 1–337) expression constructs, respectively. The HIP1wt and HIP1Δ3-5 inserts cloned into the pGEX4T.1 vector were generated by PCR amplification using the forward primer 5′-CCGGAATTCATGGATCGGATGGCCAGC-3′ and the reverse primer 5′-CCGCTCGAGACAGTCGTCGGCCGCCTGC-3′ and pcDNA3/FLHIP1 and pcDNA3/hHIP1Δ3-5/insAG as templates. Constructs were verified by sequencing. The GST-HIP1wt and GST-HIP1Δ3-5 fusion proteins were expressed in *Escherichia coli* strain BL21 after induction with 0.1 mmol/L isopropyl-L-thio-B-D-galactopyranoside (IPTG) for 2 h at 37°C. Bacteria were pelleted and resuspended in PBS containing protease inhibitors (Roche Diagnostics). Resuspended cells were lysed by sonication, and Triton X-100 was added to a final concentration of 2%. The mixture was centrifuged at 12,000×*g* for 10 min. After centrifugation, the supernatant was added to glutathione sepharose 4 beads (50% slurry) and incubated at room temperature for 30 min. The beads were washed thrice with PBS and elution buffer [50 mmol/L Tris-HCL, 10 mmol/L reduced glutathione([pH 8.0)] to elute the fusion proteins. Eluted proteins were dialyzed in PBS at 4°C for 2 h and again overnight. Dialyzed proteins were concentrated using Aquacide (Calbiochem), and protein concentrations were determined by SDS-PAGE and Coomassie blue staining. Proteins were further analyzed by Western blot analysis using an anti-GST antibody (Cell Signaling Technologies) and an anti-HIP1 antibody (UM354).

Lipid-binding assay. Lipid-binding assays using PIP strips and PIP arrays (Echelon) were performed according to manufacturer's protocol. Briefly, either PIP strips or PIP arrays were incubated overnight at 4°C with 12.5 μg of purified protein in TBST with 1% milk. Binding was detected using anti-GST antibody (1:5,000) or UM354 (1:2,000) in TBST with 1% milk. Antirabbit secondary antibodies conjugated to horseradish peroxidase were used at 1:5,000 (for anti-GST) or 1:2,000 (for UM354) in TBST with 1% milk.

Results

Germ line deletion of *Hip1* exons 3 to 5 leads to a phenotype similar to that of *Hip1*^{null} mice. The *Hip1* gene has a complex structure consisting of 32 exons spread over 220 kb. To examine the role *Hip1* plays in development and disease, we have generated a series of *Hip1* (16) and *Hip1r* (17) mutant alleles. The original *Hip1*^{null} allele was serendipitously generated in an attempt to knock the human HIP1/PDGFβR fusion cDNA into the mouse *Hip1* genomic locus (16). Using this null allele, we previously reported that HIP1 deficiency leads to a complex degenerative mouse phenotype (16) and impaired tumor progression in TRAMP mice (23). Because of the complex structure of this original allele and the resultant multitissue phenotype, we generated a conditional *Hip1* mutant allele (*Hip1*^{loxp}). To do this, we generated a targeting vector to introduce loxP sites flanking *Hip1* exons 3 to 5, which encode a significant portion (80%) of the ANTH domain. As predicted, Cre-mediated recombination of these loxP sites resulted in the deletion of exons 3 to 5, as well as the neomycin selection cassette (16). The resulting allele (*Hip1*$^{\Delta 3\text{-}5}$) contains not only a deletion of most of the ANTH domain sequences but also a frame-shifted, nonsense mutation that fuses exon 2 to exon 6. Protein expressed from this mutant allele is predicted to be a truncated amino terminal 10-kDa protein lacking the ANTH, clathrin-binding, AP2-binding, coiled coil, and Talin homology domains (domains that span the remaining 90% of the coding sequence; Fig. 1).

Previously, mice homozygous for the Δ3-5 allele were found to exhibit degenerative phenotypes similar to the *Hip1*$^{null/null}$ mice

(e.g., kypholordosis and testicular degeneration/infertility). However, there were two differences in the phenotypes associated with these mice. First, the *Hip1*$^{\Delta 3\text{-}5/\Delta 3\text{-}5}$ mice did not have cataracts. Second, the *Hip1*$^{\Delta 3\text{-}5/\Delta 3\text{-}5}$ mice did not display perinatal lethality (16). These differences suggested that either the *Hip1*$^{\Delta 3\text{-}5}$ allele is not a complete null allele or that the serendipitous *Hip1*$^{\text{null}}$ allele affects neighboring genes and that those effected genes (rather than *Hip1*) are necessary for embryogenesis and lens homeostasis.

Breast and prostate tumorigenesis is not inhibited in Hip1$^{\Delta 3\text{-}5/\Delta 3\text{-}5}$ mice. Because HIP1 is known to transform mouse fibroblasts (20) and is overexpressed in multiple human cancers (19), it has been hypothesized to play a role in tumorigenesis. We have previously shown that HIP1 deficiency inhibits prostate tumor progression in TRAMP mice (23). To examine further the involvement of HIP1 in tumor development, we analyzed the effect of HIP1 deficiency on breast tumorigenesis using the MMTV-myc mammary tumor model (24). Because of its less complex structure but similar phenotype to the *Hip1*$^{\text{null}}$ allele, we have used the *Hip1*$^{\Delta 3\text{-}5}$ allele in our subsequent studies of the role of HIP1 in tumorigenesis. MMTV-myc and TRAMP transgenic mice were generated in both the *Hip1* null and Δ3-5 genetic backgrounds. The MMTV-myc mice were sacrificed before or at 12 months of age and analyzed for the appearance and progression of breast tumors (Supplementary Fig. S1). Consistent with our previous results using the TRAMP mice, the HIP1 null background inhibited tumorigenesis induced by the MMTV-myc transgene (23), such that none of the six *Hip*$^{null/null}$;MMTV-*myc* mice (0%) analyzed developed breast tumors. In contrast, 3 of 16 *Hip*$^{+/null}$;MMTV-*myc* mice (18.8 %) analyzed developed breast tumors. This trend supports the hypothesis that HIP1 deficiency inhibits breast tumorigenesis (Fig. 2*A*).

The use of the Δ3-5 allele (compared with the null allele) to generate a HIP1-deficient background resulted in a different effect on tumorigenesis. For the MMTV-myc mice, 8 of 18 *Hip1*$^{\Delta 3\text{-}5/\Delta 3\text{-}5}$ mice (44%) and 19 of 37 *Hip1*$^{+/\Delta 3\text{-}5}$ mice (51%) developed palpable breast tumors (Fig. 2*A*). This level is significantly higher than the 19% breast tumor incidence in MMTV-myc mice with the *Hip1*$^{+/null}$ backgrounds and the 0% incidence in the *Hip1*$^{\text{null/null}}$ background (Fig. 2*A*). Additionally, we only observed breast tumor metastasis in mice that contained the Δ3-5 allele (Fig. 2*B*). Both multiple synchronous primary breast tumors (Fig. 2*C*) and multiple metastatic foci (Fig. 2*D*) were observed in *Hip1*$^{+/\Delta 3\text{-}5}$ and *Hip1*$^{\Delta 3\text{-}5/\Delta 3\text{-}5}$ mice.

The TRAMP;*Hip1*$^{\Delta 3\text{-}5}$ mice produced similar results with a smaller cohort of mice available for tumor analysis (Supplementary Fig. S2). We initially planned to compare larger groups of 6-month-old heterozygous and homozygous TRAMP;*Hip1*$^{\Delta 3\text{-}5}$ mice. This plan was based on the results of three independent prior TRAMP experiments, which showed that *Hip1*$^{\text{null/+}}$ and *Hip1*$^{+/+}$ mice developed prostate cancer at a similar frequency and to a similar extent in the TRAMP background and survived to at least 6 months of age. As expected, when we performed this fourth TRAMP experiment, we observed that 84% (15 of 18) and 93% (14 of 15) of the TRAMP mice that were heterozygous and homozygous for the null allele, respectively, survived 6 months of age (Supplementary Fig. S3*A*). Unexpectedly, *Hip1*$^{\Delta 3\text{-}5}$;TRAMP mice (both heterozygotes and homozygotes) began to die spontaneously by 4 months of age, and only 35% (5 of 14) of the homozygotes and 69% (9 of 13) of the heterozygotes survived to the 6-month point (Supplementary Fig. S3*A*). This reduction in survival associated with the *Hip1*$^{\Delta 3\text{-}5}$ allele was not due to the effects of the *Hip1*$^{\Delta 3\text{-}5/\Delta 3\text{-}5}$ degenerative phenotype (e.g., kypholordosis, dwarfism, etc.), as it was observed in both the heterozygotes and the homozygotes. In the TRAMP mice that were available for tumor analysis, we found that four of the five surviving homozygous *Hip1*$^{\Delta 3\text{-}5}$ allele–bearing TRAMP mice had gross prostate tumors (80%) and three of those four tumor-bearing mice displayed gross evidence for multiple synchronous primary tumors in different lobes of the prostate (Supplementary Fig. S3*B*). In comparison, there was no evidence for multiple primary tumors in the *Hip1*$^{\Delta 3\text{-}5/+}$ [seven of these nine (75%) mice had prostate cancer], *Hip1*$^{null/+}$ [6 of the 18 (33 %) mice had prostate cancer], or *Hip1*$^{\text{null/null}}$ [5 of the 15 (33%) had prostate cancer] TRAMP mice.

A novel cryptic splicing event allows for expression of a large mutant HIP1 protein. The difference in tumor incidence in the *Hip1*$^{\text{null/null}}$ mice and the *Hip1*$^{\Delta 3\text{-}5/\Delta 3\text{-}5}$ mice suggests either

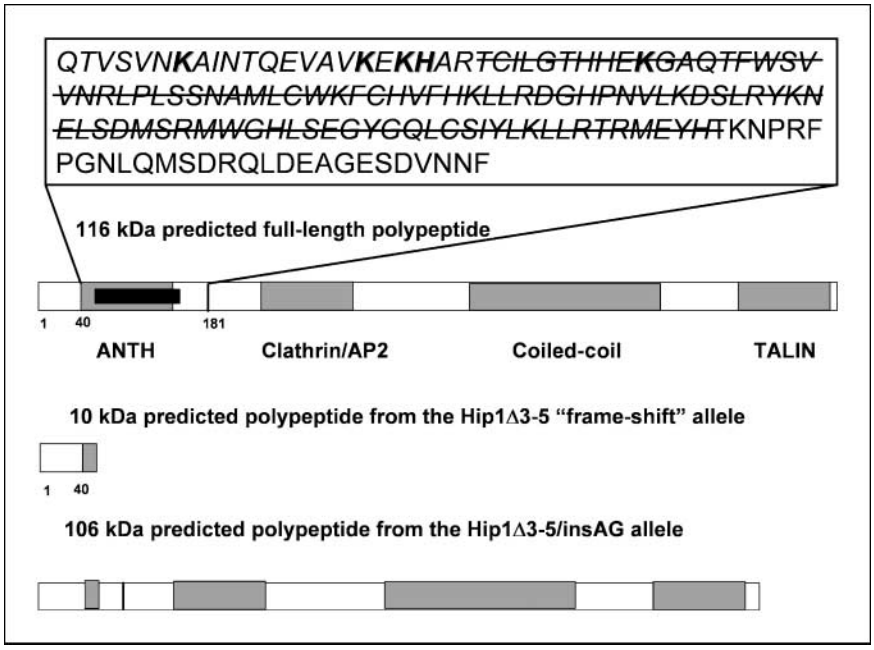

Figure 1. Amino acid sequence of the HIP1 ANTH domain and schematic diagram of the HIP1 domain structure. The majority of the mouse ANTH domain is encoded by exons 3 to 5. The amino acid sequence of the mouse ANTH domain (*italicized*; refs. 12, 13) and a few additional carboxyl amino acids are shown in the box above the schematic diagram of the full-length protein. A line is drawn through the amino acids that are encoded by exons 3 to 5. Residues (*in bold*; K, K, KH, K) share homology with AP180 and epsin and are considered to be critical inositol lipid-binding residues. The predicted protein product encoded by the *Hip1*$^{\Delta 3\text{-}5}$ allele is 10 kDa and is shown schematically below the full-length HIP1 diagram. The predicted protein product from the Hip1Δ3-5insAG cDNA is 106 kDa and is also shown schematically.

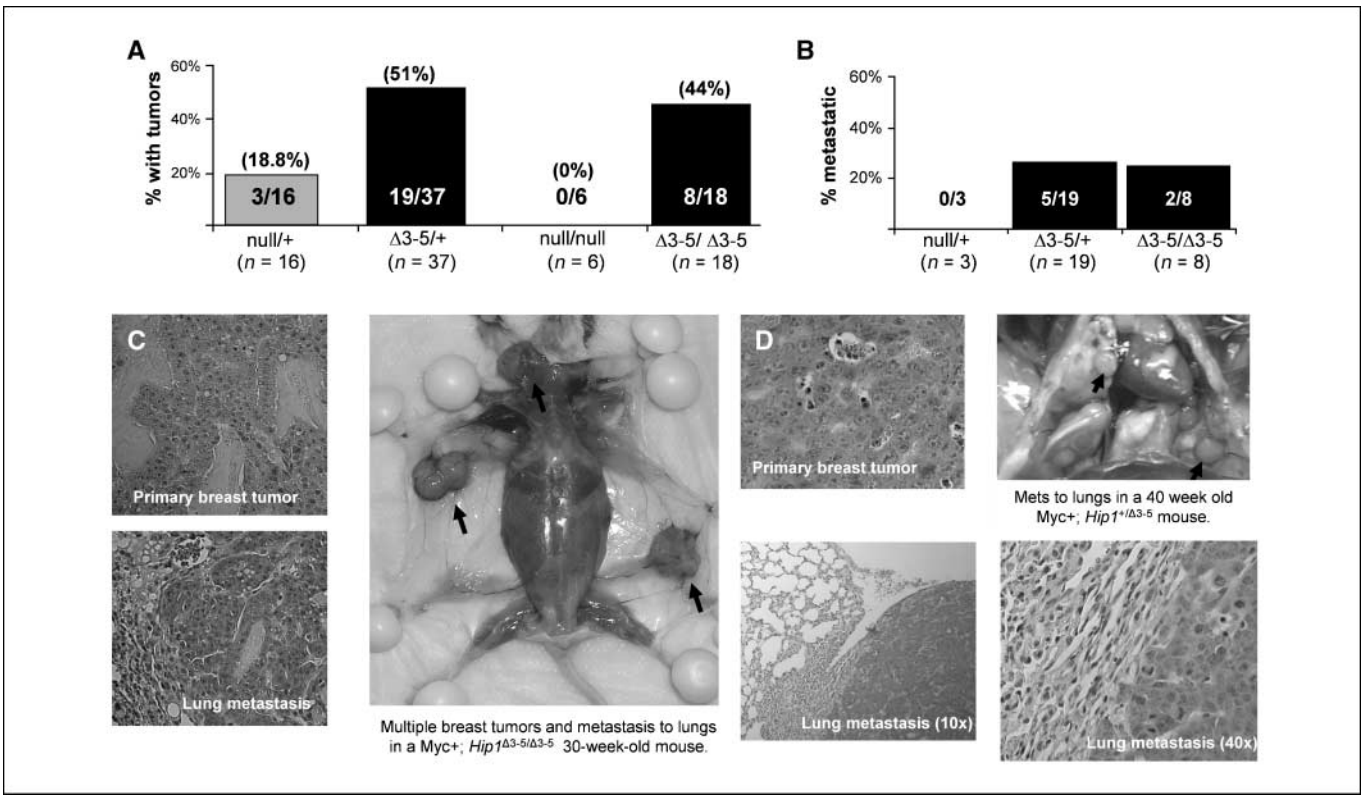

Figure 2. Breast tumorigenesis in the presence of the *Hip1*$^{\Delta 3\text{-}5}$ allele. *A,* MMTV-myc transgenic mice on different *Hip1*^{null} and *Hip1*$^{\Delta 3\text{-}5}$ genetic backgrounds were necropsied at 1 y of age or earlier if a tumor ulcerated. Forty-four percent of the Myc+;*Hip1*$^{\Delta 3\text{-}5/\Delta 3\text{-}5}$ mice developed breast tumors compared with none of the Myc+;*Hip1*$^{null/null}$ mice. Fifty-one percent of the Myc+;*Hip1*$^{+/\Delta 3\text{-}5}$ mice developed breast tumors compared with 19% of Myc+;*Hip1*$^{+/null}$ mice. *B,* none of the Myc+;*Hip1*$^{+/null}$ mice with tumors (n = 3) had metastatic tumors. Twenty-five percent of Myc+;*Hip1*$^{\Delta 3\text{-}5/\Delta 3\text{-}5}$ mice with tumors (n = 8) and 26% of Myc+;*Hip1*$^{+/\Delta 3\text{-}5}$ mice with tumors (n = 19) displayed metastasis of their breast tumors to organs, including the lungs, liver, spleen, and salivary gland. *C,* example of multiple primary breast tumors and lung metastasis in a Myc+;*Hip1*$^{\Delta 3\text{-}5/\Delta 3\text{-}5}$ 30-week-old mouse. *D,* example of lung metastasis of a breast tumor in a Myc+;*Hip1*$^{+/\Delta 3\text{-}5}$ 40-week-old mouse.

that (*a*) the original null allele alters the expression of neighboring genes and that it is those genes that influence tumorigenesis or (*b*) the Δ3-5 allele is not a completely null allele. To investigate these two possibilities, we examined normal and tumor tissues from TRAMP and MMTV-myc mice with the Δ3-5 allele for the expression of polypeptides that react with HIP1-specific antibodies. Extracts from these tissues were analyzed by Western blot for the presence of either full-length or truncated HIP1 protein using a polyclonal rabbit antibody (UM354) specific for the amino-terminal end of the HIP1 protein (Fig. 3*A, lanes 5–10*). Additionally, tumor tissue was dissociated and cultured so that tumor cells from these mice could be analyzed. Results of this analysis indicated that a truncated protein ~10 kDa smaller than the wild-type HIP1 protein was expressed in the *Hip1*$^{\Delta 3\text{-}5/\Delta 3\text{-}5}$ tumor-derived cultured cells (Fig. 3*A, lanes 1* and *2* versus *lanes 3* and *4*). Extracts derived from the bulk of the tumor, as well as other selected tissues from these mice, showed the expected lack of expression (Fig. 3*A, lanes 5–10*).

In the construction of the Δ3-5 allele, exons 3 to 5 were deleted not only to disrupt the ANTH domain but also to ensure that the splicing of exon 2 with exon 6 or any of the other exons downstream of exon 6 would result in a frame shift that would lead to premature truncation at the amino-terminal end of the protein. Therefore, the presence of a truncated HIP1 protein in these tumor cells, which is only 10 kDa smaller than the wild-type protein, was quite surprising (Fig. 3*A, lanes 3* and *4*). To identify the mRNA that encodes for this truncated HIP1 protein, we performed RT-PCR using total RNA derived from TRAMP and MMTV-myc tumor-derived cultured cells. Primers specific to the exon 1 and the exon 14/15 junctions of the HIP1 cDNA sequence (NCBL BLAST accession no. NT_039314) were used in the initial RT-PCR reaction. We detected a PCR product of the expected size (1.6 kb) in tumor-derived cells generated from wild-type mice and from mice heterozygous for the Δ3-5 allele (Fig. 3*B, lanes 2, 4,* and *6–8, WT arrow*). An additional band ~300 bp smaller (i.e., 1.3 kb) than expected was observed in both heterozygous and homozygous mice. These bands were excised from the gel and PCR amplified using nested primers, and the products were sequenced. The cDNA sequence for the nested 1.6-kb product was identical to that of the wild-type *Hip1* cDNA. Interestingly, the sequence of the nested 1.3-kb product contained exon 2 fused to exon 6 with a dinucleotide AG insertion in the junction. This dinucleotide insertion put the exon 2/6 fusion in frame (Supplementary Fig. S4) such that it encodes for an only slightly truncated HIP1 protein (Fig. 3*C*, observed sequence).

To examine further the above-described HIP1 mutant protein, we sequenced the *Hip1* gene from genomic DNA derived from cultured tumor cells. Surprisingly, we did not detect a mutation. However, careful analysis of the genomic sequence revealed two unique findings to explain the aberrant protein and transcript expression. First, we found that intron 2 uses a rare AT-AC U12-dependent splicing mechanism (Fig. 3*C*). This type of intron, which represents ~1% of the introns in the mammalian genome (27), consists of 5′AT and 3′AC splice sites. Second, we found that the

intron 5 splice acceptor (a typical AG) is immediately preceded by an AC. This ACAG sequence allows for the incorporation of an AG dinucleotide into the coding sequence of the mRNA transcript and serendipitous maintenance of the original reading frame. The predicted size of this mutant protein is 106 kDa (Fig. 1 schematic), which is very similar to the size of the observed protein product (Fig. 2*A, lanes 3* and *4*).

Mutant HIP1Δ3-5insAG protein expression in embryonic and adult lung and brain tissues. The presence of this AG dinucleotide insertion that placed exons 2 and 6 in frame in both Δ3-5 heterozygous and Δ3-5 homozygous cells led us to reevaluate whether or not *Hip1* protein is expressed in normal tissues. We isolated selected normal cells and tissues from wild-type, Δ3-5 heterozygous, and Δ3-5 homozygous mice and analyzed them for the presence of the Hip1Δ3-5insAG protein product. Using Northern blot analysis of embryonic fibroblast RNA (Fig. 4*A*), we found that the truncated message was evident in homozygous mice (*lane 2*) when analyzed beside wild-type RNA (*lane 1*). Using RT-PCR, we also found that tissue from the brains, lungs, and kidneys of Δ3-5 heterozygous and homozygous mice contained the HIP1Δ3-5insAG mRNA (Fig. 4*B*). No PCR product representing the Hip1Δ3-5 mRNA was observed in wild-type mice (Fig. 4*B, lanes 3, 6,* and *9*). We also found that extracts from cultured, early passage embryonic fibroblasts and embryonic brain contained easily detectable truncated HIP1Δ3-5insAG protein product (Supplementary Fig. S5). In contrast, nearly all adult tissues, with the exceptions of the lung and brain (Fig. 4*C, lanes 6* and *8*), displayed very low levels of HIP1 polypeptide expression (Fig. 4*C, lanes 2, 4,* and *10*; use of an amino-terminal polyclonal antibody UM354). Either the diminished expression or the lack of function of the HIP1Δ3-5insAG product could explain why these mice display a degenerative phenotype similar to that of the original homozygous null mice. In addition to the altered expression levels of the HIP1 peptides in various tissues, we noted that the migration of the HIP1 protein in the embryonic brain was quite different from that in the adult brain. Analysis of the *Hip1* protein product in embryonic, newborn, preweaned, and adult mice indicated that this differential expression correlates with developmental stage, with the product in the adult brain migrating distinctly slower or comigrating with the wild-type form of HIP1 (Fig. 4*D, lanes 2, 4,* and *6*). The molecular explanation of this striking developmental correlation remains to be determined.

Next, using the original $Hip1^{loxp/loxp}$ mice (16), we generated a tissue-specific Δ3-5 recombinant allele. By crossing the $Hip1^{loxp}$ mice with mice carrying an IFN inducible Mx1-Cre transgene, we generated mice that expressed the Δ3-5 allele only in cells of the

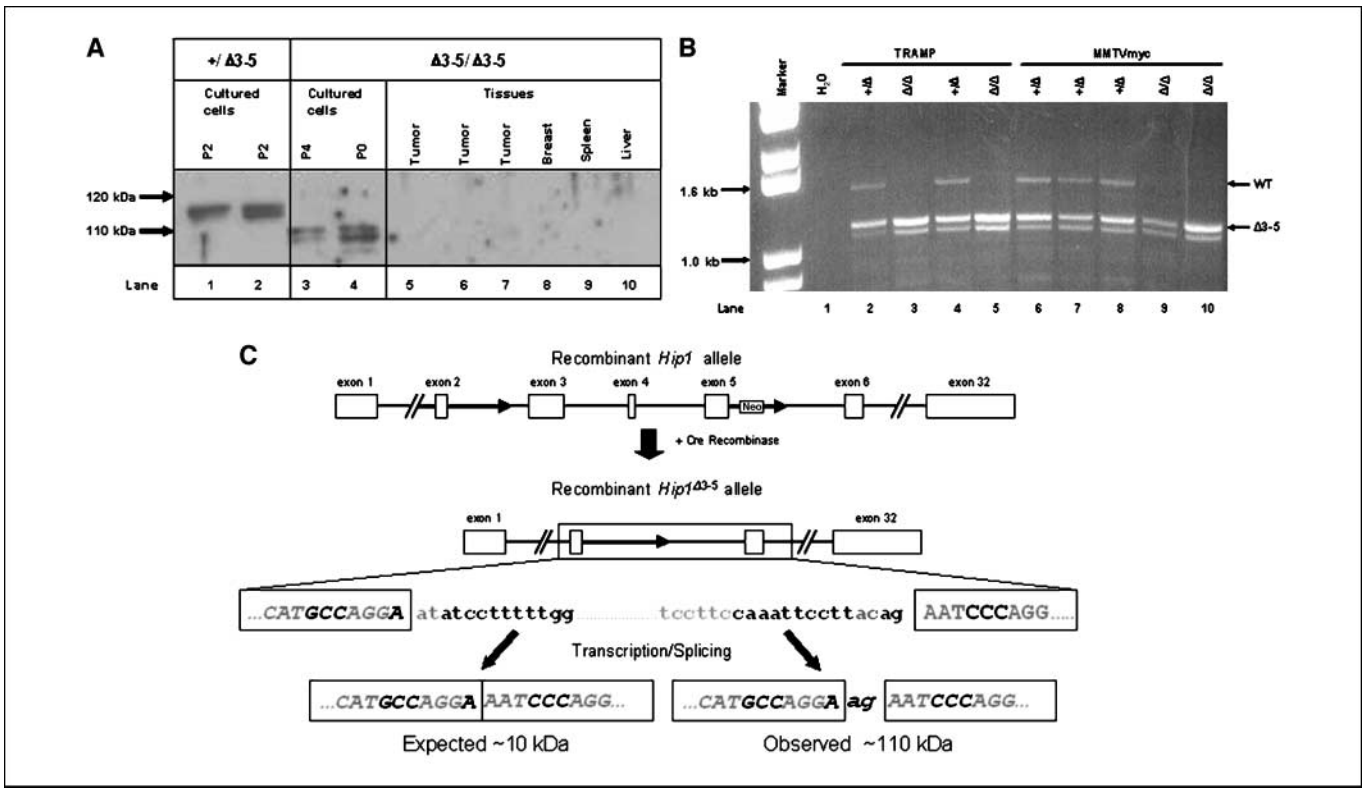

Figure 3. Expression of HIP1 sequences in HIP1Δ3-5 mice. *A,* tumors from mice with breast (MMTV-myc) and prostate (TRAMP) cancer were grown in culture and analyzed by Western blot for the presence of HIP1 polypeptides. Results from an MMTV-myc breast tumor sample. *P*, passage number. Even at zero passages (*P0*), the cultured cells from Δ3-5/Δ3-5 tumors expressed a slightly truncated form of HIP1 (*lane 4*). This product was not detected in the bulk tumor tissue, in the normal tissues tested of these mice, or in any cell types derived from mice heterozygous for the Δ3-5 allele (*lanes 5–10*). *B,* RT-PCR of total RNA extracted from Δ3-5 allele–containing tumor-derived cultured cells resulted in the generation of wild-type (*WT*) and mutant (Δ3-5) bands of expected sizes. *C,* partial Hip1Δ3-5 cDNA sequence alignment with wild-type mouse Hip1 cDNA showed an AG dinucleotide insertion between exons 2 and 6 of the Hip1Δ3-5 cDNA sequence. This insertion maintains the open reading frame of the transcript. Tumor cell line genomic DNA contains a recombined AT-AC intron. Genomic DNA isolated from a Myc breast tumor–derived cell line was sequenced in the region where the recombination occurred (*box*). The sequence was compared with wild-type *Hip1* genomic DNA, and no additional mutations were observed. Note the recombinant intron flanked by exons 2 and 6 has a U12-dependent consensus branch point sequence (*italicized*) and a 3′ AC dinucleotide (*italicized*) that serves as the cryptic splice site acceptor. This splicing event results in an AG insertion in the transcript. The region sequenced is indicated by the box that encompasses exon 2, exon 6, and intervening sequences, including the single loxP site.

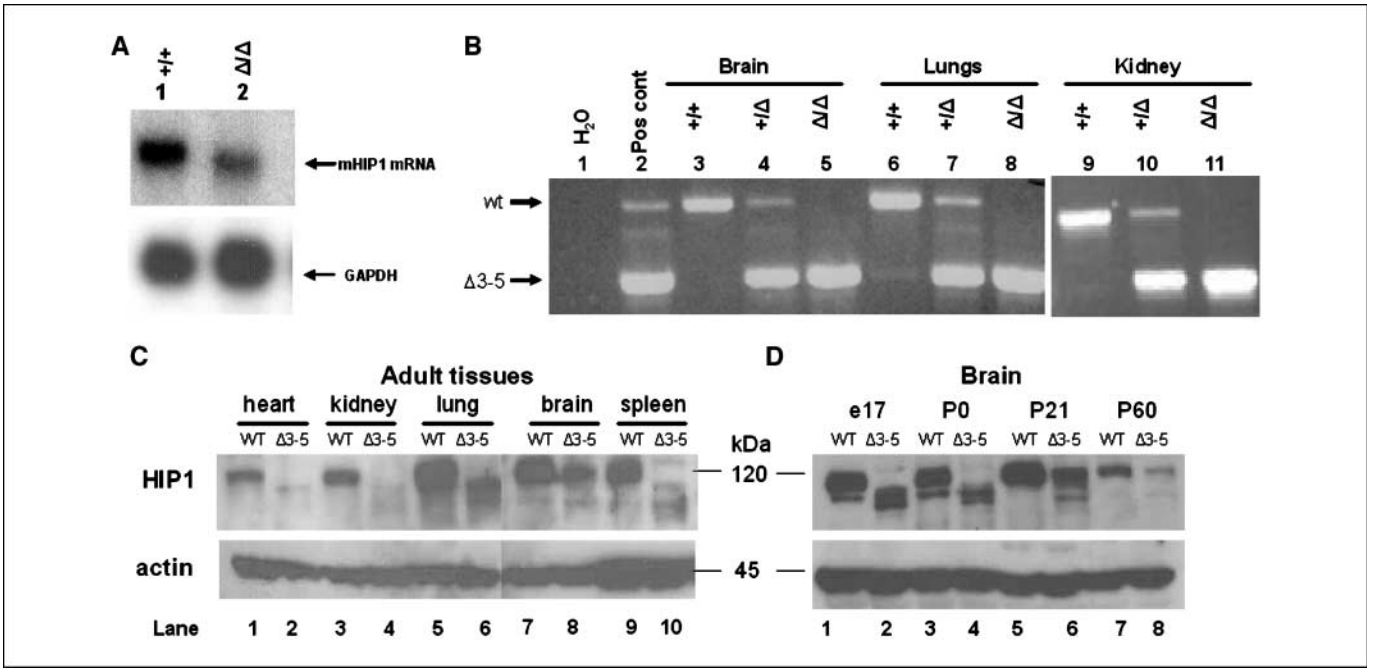

Figure 4. Expression patterns of the Δ3-5insAG mRNA and its putative protein product. *A,* Northern blot analysis using a probe specific for the 5′ end of the mouse Hip1 mRNA (nucleotides 1–1260) showed the presence of a significant amount of a slightly truncated product in the RNA of mouse embryonic fibroblast (*lane 2* versus *lane 1*). *B,* primers specific to the exon 1/2 junction (forward) and the exon 13/14 junction (reverse primer) of murine *Hip1* cDNA were used to amplify the cDNA. The resulting products were separated on a 1.0% agarose gel. Water was used as the negative control (*lane 1*). RNA from a TRAMP prostate cancer cell line generated from the prostate tumor tissue of a mouse that was heterozygous for the $Hip1^{\Delta 3\text{-}5}$ allele was used as a positive control for both the wild-type *Hip1* and $Hip1\Delta^{3\text{-}5/insAG}$ mRNA transcripts (*lane 2*). A 1.6-kb band indicates the presence of wild-type *Hip1* mRNA transcripts, whereas a 1.3-kb band indicates the presence of the mutant $Hip1\Delta^{3\text{-}5/insAG}$ mRNA transcripts. Brain, lung, and kidney tissues from wild-type *Hip1* mice (+/+) produced the 1.6-kb band, but not a 1.3-kb band (*lanes 3, 6,* and *9*). Similar tissues from heterozygous Δ3-5 mice (+/Δ) produced both a 1.6-kb band and a 1.3-kb band (*lanes 4, 7,* and *10*). Only the 1.3-kb band was produced in brain, lung, and kidney tissues from homozygous Δ3-5 mice (Δ/Δ; *lanes 5, 8,* and *11*). *C,* expression of the truncated product was most prominent in lung tissue, although lesser amounts are detected in all other tissues tested. Interestingly, brain tissue from Δ3-5 adult mice displayed significant amounts of a protein product that comigrated with the wild-type form. This comigration was not observed in the extracts from embryonic brains (described in *D*). Actin blotting was performed using an anti-actin monoclonal antibody (Sigma) as a control. *D,* postnatal day 0 brains (isolated immediately after birth) have HIP1-banding patterns similar to those of embryos. Preweaning stage brains have two distinct HIP1 bands, and the adult brains have a HIP1 band that comigrates with the wild-type band.

adult hematopoietic system, liver, and kidney after pIpC-mediated induction of Cre expression (26, 28). With these mice, we examined whether the gross phenotype of the germ line Δ3-5 mouse could be recapitulated only in the isolated adult tissues. Interestingly, Western blot analysis of extracts from the spleen, liver, kidney (Fig. 5*A*), and bone marrow (Fig. 5*B*) of Mx1-Cre–induced mice showed that the expression of the truncated HIP1 protein was most prominent in the spleen (Fig. 5*A, lanes 9–11*) and bone marrow (Fig. 5*B, lanes 3, 5, 7,* and *8*) and loss of HIP1 expression altogether was frequently observed in the normal liver (*lane 4–6, panel 1*) and kidney (Fig. 5*A, lanes 9–11, panel 4*), but as expected not in brain, heart, eye (Fig. 5*A*), uterus, ovary, or the gastrointestinal tract (data not shown). It is of interest that the two tissues, liver and kidney, where we observed HIP1 protein deficiency due to a complete recombination event did not display the degenerative phenotype observed in the germ line recombined Δ3-5 mice. We, therefore, conclude that tissue-specific HIP1 deficiency in the liver and kidney does not induce the knockout phenotype. Unfortunately, we could not make this conclusion in the hematopoietic system, as despite repeated attempts to induce IFN with pIpC, the complete recombination of the $Hip1^{loxp}$ allele in the Mx1-Cre mice was not achieved in hematopoietic tissues (Fig. 5*B, lane 7*) and, therefore, a significant amount of wild-type Hip1 expression remained in the homozygotes.

These findings also suggest the possibility that the truncated HIP1 protein may be preferentially expressed in dividing cells, including tumorigenic cells. This prediction is supported by the finding that Δ3-5insAG protein was present in the fibroblasts and brains of Δ3-5 mouse embryos at E17.0 day (Fig. 4*C, lanes 5, 6, 11,* and *12*). Furthermore, we discovered a gross liver tumor in an Mx1-Cre;$Hip1^{loxp/+}$ mouse (Fig. 5*C*). The tumor from this mouse expressed a truncated Δ3-5 protein product, whereas the surrounding normal liver did not. Additionally, we identified a trend in which the spleen sizes of the *Hip1*-floxed, Mx1-Cre, pIpC-treated mice increased, although frank hematopoietic malignancies were not observed (data not shown).

The HIP1Δ3-5insAG protein retains its ability to bind lipids, clathrin, AP2, and EGFR. We have observed some slight phenotypic differences between the $Hip1^{\Delta 3\text{-}5/\Delta 3\text{-}5}$ mice and the $Hip1^{null/null}$ mice (16). These differences included absence of cataracts or perinatal death in the $Hip1^{\Delta 3\text{-}5/\Delta 3\text{-}5}$ mice, increased mortality from tumors in the TRAMP;$Hip1^{\Delta 3\text{-}5}$ mice relative to the TRAMP;$Hip1^{null/null}$ mice (Supplementary Fig. S3*A*), no decrease in breast or prostate tumorigenesis in $Hip1^{\Delta 3\text{-}5}$ allele–bearing backgrounds (although there was a trend toward more tumors; Fig. 2*A*), and a liver tumor in a young, conditional $Hip1^{\Delta 3\text{-}5}$ heterozygous mouse (Fig. 5*C*). Given these differences, we examined whether the Hip1Δ3-5insAG protein product possesses all or a subset of its cellular activities that promote normal and neoplastic cell proliferation/survival by assessing its ability to bind to lipids, endocytic factors, and EGFR.

Because this truncated protein retains its clathrin-binding, AP2-binding, and EGFR-binding regions, we predicted that the

Hip1Δ3-5insAG protein product would have the ability to bind these proteins. To test this hypothesis, we expressed the *HIP1*$\Delta^{3\text{-}5/insAG}$ cDNA in 293T cells, immunoprecipitated the mutant protein with an anti-HIP1 polyclonal antibody (UM323, bleed 8/2002), and immunoblotted the precipitates to determine the presence or absence of the endocytic proteins and EGFR. As expected, the truncated mutant protein–bound EGFR, clathrin, and AP2 (the α subunit; Fig. 6*A, lanes 11* and *15*). In contrast, expression of a human HIP1 mutant cDNA construct that lacks the AP2-binding and clathrin-binding domains did not bind these endocytic proteins (Fig. 6*A, lanes 12* and *16*). Also, it should be noted that the interaction between HIP1 and EGFR was apparently enhanced by the deletion of either the sequences encoded for by exons 3 to 5 (Fig. 6*A, lanes 11* and *15* compared with *lanes 10* and *14*) or the domains that bind to endocytic proteins (Fig. 6*A, lanes 12* and *16*), suggesting that the interaction of HIP1 with EGFR is not indirectly mediated by its binding with clathrin and/or AP2.

Because 80% of the sequence of the lipid-binding ANTH domain is deleted from the HIP1Δ3-5insAG protein (Fig. 1), we predicted that this mutant would not likely retain its lipid-binding activity. Interestingly, most of the key residues that are important for the direct binding of the ANTH domain–containing proteins to PtdIns(4,5)P_2 were retained in the Δ3-5 protein product (key residues are bold in Fig. 1; refs. 12, 13). However, one key residue (homologous to K76 of epsin) that has been shown to be important in binding to the Ins(1,4,5)P_3 head group (13) is deleted in the truncated Δ3-5 protein. To determine whether the Δ3-5 protein product retained its lipid-binding capacity, we examined lipid binding using recombinant GST-HIP1^{wt} and GST-HIP1$\Delta^{3\text{-}5/insAG}$ fusion proteins. We generated and glutathione-Sepharose purified GST fusion proteins that contained the first 430 and 370 amino

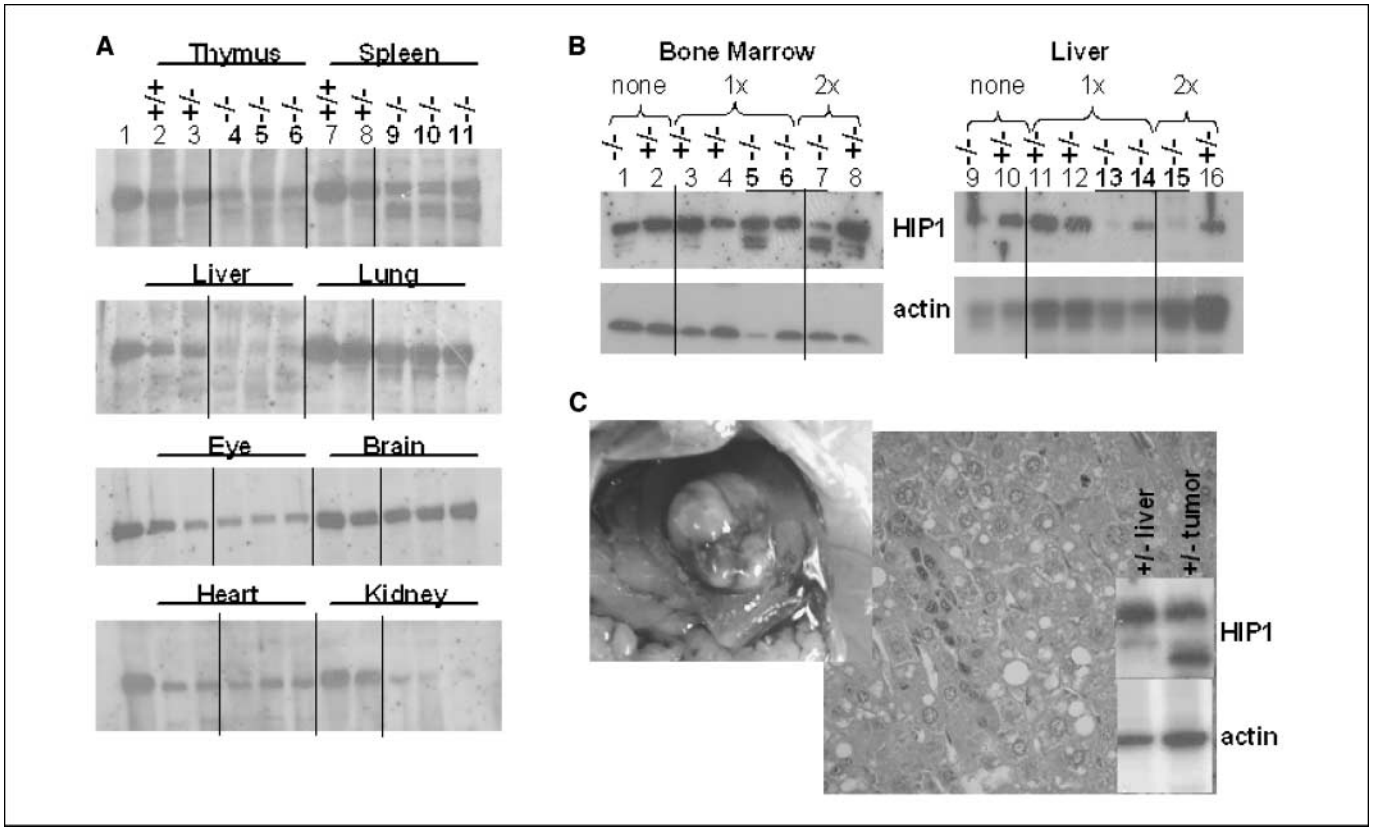

Figure 5. Conditional Cre-mediated recombination of the floxed *Hip1* allele leads to either HIP1 deficiency or expression of the truncated product depending on tissue analyzed. *A,* Mx1-Cre transgenic mice carrying none (+/+; *lanes 2* and *7*), one (−/+; *lanes 3* and *8*), or two (−/−; *lanes 4–6* and *9–11*) of the floxed *Hip1* alleles were treated with three injections of pIpC at 8 to 12 wk of age and then were retreated at 20 wk of age. Their organs were harvested at 28 to 32 wk of age. Organ extracts were separated on 6% SDS-PAGE and analyzed for HIP1 expression by Western blotting [using the UM354 (1:5,000) antibody]. An extract of a wild-type brain (*lane 1*) was included as a positive control of HIP1 expression. Near-complete recombination (resulting in the deficiency of HIP1 protein) was observed in liver and kidney, but not in thymus and spleen where residual wild-type HIP1 and truncated HIP1 (putative Δ3-5insAG product) was expressed. As expected, eye, brain, and heart tissue showed no evidence for recombination because Mx1-Cre is not induced in these tissues (26). A small amount of putative Δ3-5insAG truncated product was observed in lung tissue and may be a result of recombination in tissue macrophages, which are abundant in the lung tissue. *B,* mice were untreated (*lanes 1, 2, 9,* and *10*) or treated at 6 wk of age with pIpC (six doses i.p. every other day; *lanes 3–6* and *11–14*). A small group was treated with pIpC again at 20 wk of age (three additional doses every other day; *lanes 7, 8, 15,* and *16*). The mice were sacrificed at 6 mo of age, and their tissues were analyzed for HIP1 expression by Western blot (UM354). Complete deficiency of HIP1 was never observed in bone marrow despite continued pIpC injections, whereas complete deficiency of HIP1 was achieved and maintained in the liver without repeated recombination. Interestingly, in the mouse without complete recombination in the liver (*lane 14*), there was no truncated product in its cultured bone marrow (*lane 6*). A small amount of the truncated product was observed in cultured bone marrow from some untreated mice (e.g., *lane 1*), a finding consistent with the possibility that the endogenous production of IFN (i.e., in response to viral infections) can activate Mx1-Cre expression at low levels in mice in the absence of pIpC treatment. As a loading control, actin blots were performed on 10% SDS-PAGE using a monoclonal anti-actin antibody (Sigma). *C,* mice were treated with pIpC in two stages: first at 21 wk of age (with six every-other-day doses) and second at 55 wk of age (with six every-other-day doses). Six treated mice (three heterozygous and three homozygous) and five untreated mice were necropsied. At necropsy, a previously undetected liver tumor was discovered in a treated heterozygous mouse, and it was harvested for histologic and protein expression analysis. Increased amounts of truncated HIP1 expression were observed in the tumor tissue compared with surrounding normal liver tissue. Because this was a heterozygous mouse, expression from the wild-type allele was also detected.

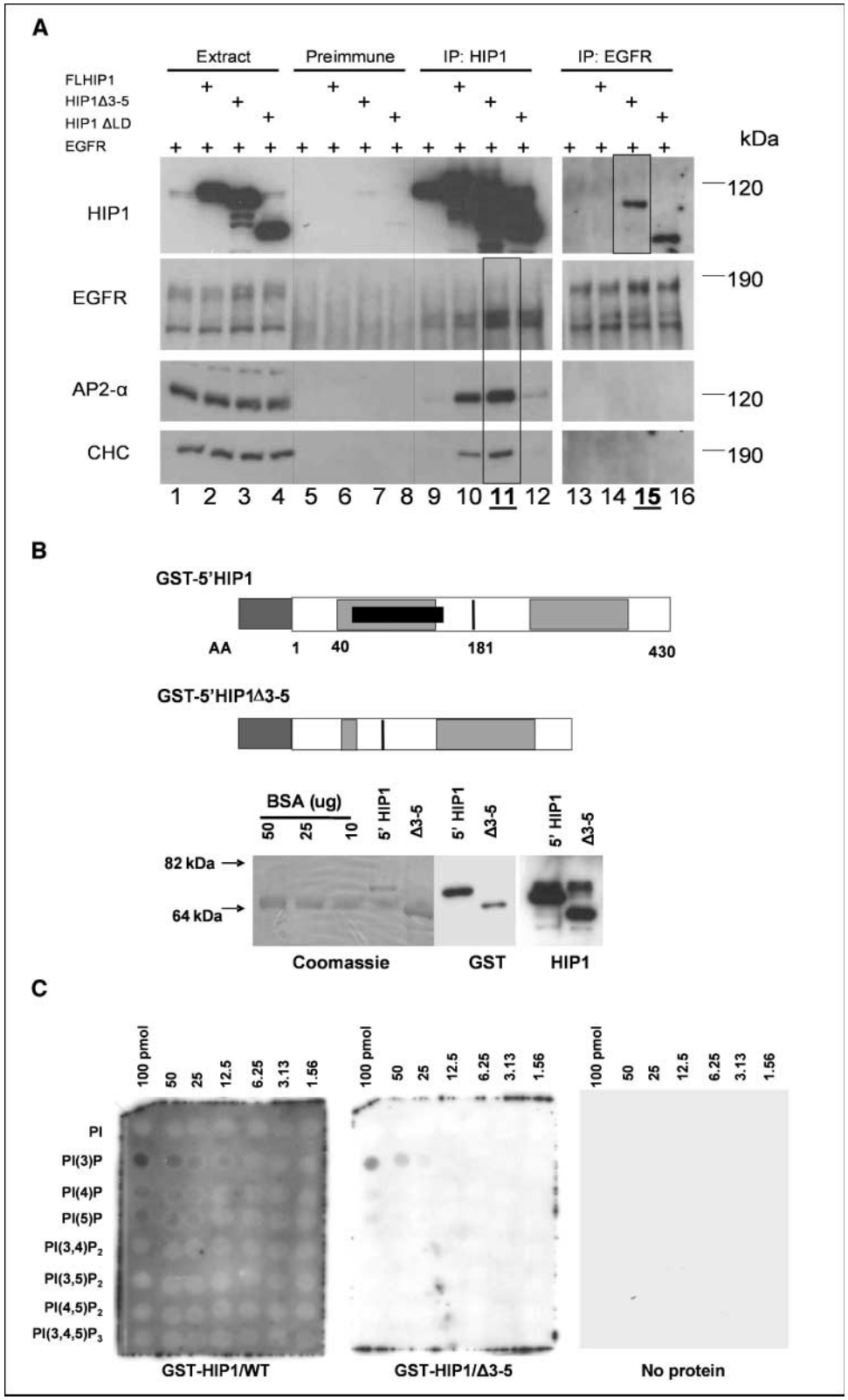

Figure 6. HIP1Δ3-5insAG association with clathrin, AP2, EGFR, and lipids. *A,* HEK 293T cells were transfected with EGFR and/or various HIP1 constructs. Cells were lysed 24 h posttransfection, and polyclonal anti-HIP1 (UM323) and anti-EGFR antibodies were used for immunoprecipitation. The immunoprecipitates were separated on 6% SDS-PAGE gels and transferred to nitrocellulose for Western blot analysis using the indicated antibodies. *Lanes 1-4,* whole-cell lysates; *lanes 5-8*, preimmune immunoprecipitates; *lanes 9-12*, anti-HIP1 immunoprecipitates; *lanes 13-16*, anti-EGFR immunoprecipitates. Note the association of AP2, CHC, and EGFR with HIP1 is preserved despite deletion of sequences encoded by exons 3 to 5. Interestingly, the anti-EGFR antibody did not coprecipitate wild-type HIP1 (*top; lane 14*) but did coprecipitate the HIP1Δ3-5 and HIP1ΔLD mutant proteins (*top; lanes 15 and 16*). *B,* schematic diagrams of GST-5′HIP1 and GST-5′HIP1/Δ3-5 fusion proteins. Expression of these fusion proteins in *E. coli* BL21 was induced by treatment with 0.1 mmol/L IPTG. The cells were pelleted and lysed, and the fusion proteins were purified from the resulting extracts using glutathione-Sepharose 4 beads. Ten microliters of a 1:10 dilution of the purified GST-5′HIP1 and GST-5′HIP1/Δ3-5 fusion proteins were run on a 10% polyacrylamide gel and immunoblotted with an anti-GST antibody (1:5,000) or an anti-HIP1 antibody (UM354; 1:2,000) to ensure reaction of the proteins by the respective antibodies and to confirm their purity. Similar amounts were run on a separate 10% polyacrylamide gel along with various known concentrations of bovine serum albumin, and the gel was Coomassie stained to estimate the concentrations of the purified fusion proteins. *C,* protein solutions containing 10 μg of either purified GST-5′HIP1 or GST-5′HIP1/Δ3-5 protein in TBST with 1% milk were incubated with PIP arrays (Echelon) containing various concentrations of different phosphoinositides. As with the PIP strips, both GST-5′HIP1 and GST-5′HIP1/Δ3-5 proteins bound preferentially to PtdIns(3)P. Lipid-protein interactions were detected using a polyclonal anti-GST antibody (Cell Signaling Technologies). No signal was detected using antibody alone.

acids of the $HIP1^{wt}$ and $HIP1\Delta^{3\text{-}5/insAG}$ proteins, respectively (Fig. 6*B*). The purified proteins were separated by SDS-PAGE and Coomassie stained to quantitate the amount of recombinant protein. The purified recombinant proteins were also analyzed by Western blot to ensure interaction with anti-GST and anti-HIP1 antibodies (Fig. 6*B*). Next, the purified proteins were incubated with Echelon-generated PIP strips to examine whether the fusion proteins were capable of binding lipids. Both the wild-type and the $HIP1\Delta^{3\text{-}5/insAG}$ mutant fusion proteins bound PtdIns(3)P predominantly (Supplementary Fig. S6). These results were confirmed

using PIP arrays (Echelon), which were used to further examine the differential abilities of these proteins to bind to lipids. Interestingly, these truncated fusion proteins displayed a higher specific binding to PtdIns(3)P than to polyphosphorylated inositol lipids. On the other hand, our previous studies using the full-length HIP1 expressed in 293T cells indicated that its lipid-binding preference was polyphosphorylated 3-phosphoinositides (29). Our contradictory results may be due to either the absence of the carboxyl terminal end of the protein, differences in proteins expressed in bacteria versus mammalian cells, or differences in the materials used in the various assays. Additional biochemical analyses are necessary to clarify this issue. Nevertheless, the specific inositol lipid-binding capacity of the ANTH domain is retained in the Hip1Δ3-5insAG protein.

Discussion

We have previously shown that the HIP1 family of proteins are biologically important because both single *Hip1* (15, 16) and double *Hip1/Hip1r* (14) knockout mice have adult degenerative phenotypes and HIP1 protein expression is altered in multiple cancers (19). However, the exact function of this protein family remains unclear, and more detailed cellular and biochemical analyses are needed to validate predicted functions and identify novel ones. In the current study, we describe a novel form of HIP1 that is expressed *in vivo* as the result of a novel cryptic splice event between a 5′ AT-AC intron (intron 2) and a 3′ GT-AG intron (intron 5). These results are important for both technical and functional reasons. First, it illustrates an unpredicted cryptic splicing event in a previously predicted loss of function gene targeting event, and, second, this type of cellular natural selection may provide clues to the function of HIP1 in normal and neoplastic cells.

The technical aspects of these findings have provided us a very important lesson. The targeting event that we initially designed led to a mutation in the AT-AC intron 2. The rare splicing event that we observed reflects preferential splicing between splice sites of the same class. The identification of rare U12-dependent intron splicing sites or AT-AC introns will be important for all proteins with similar genetic structures (27). This finding has also raised an intriguing possibility that such splicing events might occur in normal cells leading to the expression of unexpected polypeptides. Interestingly, the rare AT-AC intron 2 is conserved in both the human and mouse *Hip1* genes. This observation is consistent with previous reports that U12-type introns are usually conserved phylogenetically (30). It has been reported previously that genes with nonredundant, crucial cellular activities may have strong selective evolutionary pressure against the conversion of U12 to U2 type introns and, therefore, have retained them. HIP1 supports this assertion as HIP1 clearly has nonredundant, crucial activities as evidenced by the fact that its deletion in mice leads to dramatic adult phenotypes (14–16).

In terms of HIP1 function, it is evident that the expression of the truncated mutant protein in adult lung and brain tissue does not prevent the adult degenerative phenotypes, such as kypholordosis or testicular degeneration. The discovery here of concomitant expression of HIP1 sequences in the Hip1Δ3-5 homozygous mice and the degenerative phenotype suggests that this mutant protein may not be completely functional in normal cells. In contrast, the presence of the truncated mutant protein in tumor cells may explain why tumorigenesis is not inhibited by the homozygosity of this allele. This proposal is supported by the finding that this mutant protein retains some of its functions (i.e., the ability to bind to lipids, clathrin, AP2, and EGFR). These findings illustrate a prototypical example that provides insights into how mouse modeling may lead to insertion mutations and unpredicted active protein products.

The maintenance of AP2-binding, CHC-binding, EGFR-binding, and lipid-binding functions in the truncated mutant HIP1 protein suggests that another HIP1 cellular function must contribute to the gross phenotype of the mutant mice. This unknown function likely explains why we were unable to identify endocytic defects in either of the mutant mouse systems. Future studies are required to understand the molecular modifications and sequences of the various forms of HIP1 that are expressed in different tissues at different times during mammalian development and how these different forms affect HIP1 functions.

Acknowledgments

Received 10/16/2007; revised 12/4/2007; accepted 12/14/2007.

Grant support: Department of Defense Idea BC031604, National Cancer Institute grants R01 CA82363-03 and R01 CA098730-01, and Susan B. Komen Foundation predoctoral award (S.V. Bradley).

The costs of publication of this article were defrayed in part by the payment of page charges. This article must therefore be hereby marked *advertisement* in accordance with 18 U.S.C. Section 1734 solely to indicate this fact.

T.S. Ross is a Leukemia and Lymphoma Society Scholar.

We thank Dr. Miriam Meisler and the Ross laboratory members for their constructive, intellectual input and for the critical review of this manuscript.

References

1. Kalchman MA, Koide HB, McCutcheon K, et al. HIP1, a human homologue of *S. cerevisiae* Sla2p, interacts with membrane-associated huntingtin in the brain. Nat Genet 1997;16:44–53.
2. Wanker EE, Rovira C, Scherzinger E, et al. HIP-I: a huntingtin interacting protein isolated by the yeast two-hybrid system. Hum Mol Genet 1997;6:487–95.
3. Engqvist-Goldstein AE, Kessels MM, Chopra VS, Hayden MR, Drubin DG. An actin-binding protein of the Sla2/Huntingtin interacting protein 1 family is a novel component of clathrin-coated pits and vesicles. J Cell Biol 1999;147:1503–18.
4. Engqvist-Goldstein AE, Warren RA, Kessels MM, Keen JH, Heuser J, Drubin DG. The actin-binding protein Hip1R associates with clathrin during early stages of endocytosis and promotes clathrin assembly *in vitro*. J Cell Biol 2001;154:1209–23.
5. Hackam AS, Yassa AS, Singaraja R, et al. Huntingtin interacting protein 1 induces apoptosis via a novel caspase-dependent death effector domain. J Biol Chem 2000;275:41299–308.
6. Legendre-Guillemin V, Metzler M, Charbonneau M, et al. HIP1 and HIP12 display differential binding to F-actin, AP2, and clathrin: identification of a novel interaction with clathrin-light chain. J Biol Chem 2002;277:19897–904.
7. Metzler M, Legendre-Guillemin V, Gan L, et al. HIP1 functions in clathrin-mediated endocytosis through binding to clathrin and adaptor protein 2. J Biol Chem 2001;276:39271–6.
8. Mishra SK, Agostinelli NR, Brett TJ, Mizukami I, Ross TS, Traub LM. Clathrin- and AP-2-binding sites in HIP1 uncover a general assembly role for endocytic accessory proteins. J Biol Chem 2001;276:46230–6.
9. Rao DS, Chang JC, Kumar PD, et al. Huntingtin interacting protein 1 Is a clathrin coat binding protein required for differentiation of late spermatogenic progenitors. Mol Cell Biol 2001;21:7796–806.
10. Waelter S, Scherzinger E, Hasenbank R, et al. The huntingtin interacting protein HIP1 is a clathrin and α-adaptin-binding protein involved in receptor-mediated endocytosis. Hum Mol Genet 2001;10:1807–17.
11. Bradley SV, Holland EC, Liu GY, Thomas D, Hyun TS, Ross TS. Huntingtin interacting protein 1 is a novel brain tumor marker that associates with epidermal growth factor receptor. Cancer Res 2007;67:3609–15.
12. Ford MG, Pearse BM, Higgins MK, et al. Simultaneous binding of PtdIns(4, 5)P2 and clathrin by AP180 in the nucleation of clathrin lattices on membranes. Science 2001;291:1051–5.
13. Itoh T, Koshiba S, Kigawa T, Kikuchi A, Yokoyama S, Takenawa T. Role of the ENTH domain in phosphatidylinositol-4,5-bisphosphate binding and endocytosis. Science 2001;291:1047–51.
14. Bradley SV, Hyun TS, Oravecz-Wilson KI, et al. Degenerative phenotypes caused by the combined deficiency of murine HIP1 and HIP1r are rescued by human HIP1. Hum Mol Genet 2007;16:1279–92.
15. Metzler M, Li B, Gan L, et al. Disruption of the

endocytic protein HIP1 results in neurological deficits and decreased AMPA receptor trafficking. EMBO J 2003; 22:3254–66.
16. Oravecz-Wilson KI, Kiel MJ, Li L, et al. Huntingtin Interacting Protein 1 mutations lead to abnormal hematopoiesis, spinal defects and cataracts. Hum Mol Genet 2004;13:851–67.
17. Hyun TS, Li L, Oravecz-Wilson KI, et al. Hip1-related mutant mice grow and develop normally but have accelerated spinal abnormalities and dwarfism in the absence of HIP1. Mol Cell Biol 2004;24: 4329–40.
18. Ross TS, Bernard OA, Berger R, Gilliland DG. Fusion of Huntingtin interacting protein 1 to platelet-derived growth factor β receptor (PDGFβR) in chronic myelomonocytic leukemia with t(5;7)(q33;q11.2). Blood 1998; 91:4419–26.
19. Rao DS, Hyun TS, Kumar PD, et al. Huntingtin-interacting protein 1 is overexpressed in prostate and colon cancer and is critical for cellular survival. J Clin Invest 2002;110:351–60.
20. Rao DS, Bradley SV, Kumar PD, et al. Altered receptor trafficking in Huntingtin interacting protein 1-transformed cells. Cancer Cell 2003;3:471–82.
21. Bradley SV, Smith MR, Hyun TS, et al. Aberrant HIP1 in Lymphoid Malignancies. Cancer Res 2007;67:8923–31.
22. Greenberg NM, DeMayo F, Finegold MJ, et al. Prostate cancer in a transgenic mouse. Proc Natl Acad Sci U S A 1995;92:3439–43.
23. Bradley SV, Oravecz-Wilson KI, Bougeard G, et al. Serum antibodies to huntingtin interacting protein-1: a new blood test for prostate cancer. Cancer Res 2005;65: 4126–33.
24. Leder A, Pattengale PK, Kuo A, Stewart TA, Leder P. Consequences of widespread deregulation of the c-myc gene in transgenic mice: multiple neoplasms and normal development. Cell 1986;45:485–95.
25. Higuchi M, O'Brien D, Kumaravelu P, Lenny N, Yeoh EJ, Downing JR. Expression of a conditional AML1-ETO oncogene bypasses embryonic lethality and establishes a murine model of human t(8;21) acute myeloid leukemia. Cancer Cell 2002;1:63–74.
26. Kuhn R, Schwenk F, Aguet M, Rajewsky K. Inducible gene targeting in mice. Science 1995;269:1427–9.
27. Patel AA, Steitz JA. Splicing double: insights from the second spliceosome. Nat Rev Mol Cell Biol 2003;4: 960–70.
28. Gu H, Marth JD, Orban PC, Mossmann H, Rajewsky K. Deletion of a DNA polymerase β gene segment in T cells using cell type-specific gene targeting. Science 1994;265:103–6.
29. Hyun TS, Rao DS, Saint-Dic D, et al. HIP1 and HIP1r stabilize receptor tyrosine kinases and bind 3-phosphoinositides via epsin N-terminal homology domains. J Biol Chem 2004;279:14294–306.
30. Burge CB, Padgett RA, Sharp PA. Evolutionary fates and origins of U12-type introns. Mol Cell 1998;2:773–85.

Use of a Cryptic Splice Site for the Expression of Huntingtin Interacting Protein 1 in Select Normal and Neoplastic Tissues

Chiron W. Graves, Steven T. Philips, Sarah V. Bradley, et al.

Cancer Res 2008;68:1064-1073.